A STUDY ON FATIGUE BEHAVIOUR OF BEAM COLUMN JOINT UNDER LOW EARTHQUAKE LOADING

WAN ZURAIMI BIN WAN HANAFI

CIVIL ENGINEERING
UNIVERSITI TEKNOLOGI PETRONAS
JULY 2009

A Study on Fatigue Behaviour of Beam Column Joint Under Low Earthquake Loading

by

Wan Zuraimi Bin Wan Hanafi

Dissertation submitted in partial fulfillment of
the requirements for the
BACHELOR OF ENGINEERING (Hons)
(CIVIL ENGINEERING)

JULY 2009

Universiti Teknologi PETRONAS

Bandar Seri Iskandar

31750 Tronoh

Perak Darul Ridzuan

CERTIFICATION OF APPROVAL

A Study on Fatigue Behaviour of Beam Column Joint Under Low Earthquake Loading

by

Wan Zuraimi Bin Wan Hanafi

A project dissertation submitted to the
Civil Engineering Programme
Universiti Teknologi PETRONAS
in partial fulfillment of the requirements for the
BACHELOR OF ENGINEERING (HONS)
(CIVIL ENGINEERING)

Approved by,

.....

(Nabilah Bt. Abu Bakar)

Supervisor

UNIVERSITI TEKNOLOGI PETRONAS

TRONOH, PERAK

July 2009

CERTIFICATION OF ORIGINALITY

This is to certify that I am responsible for the work submitted in this project, that the original work is my own except as specified in the references, and that the original work contained herein have not been undertaken or done by unspecified sources or persons.

.....

(WAN ZURAIMI WAN HANAFI)

ABSTRACT

This report is a brief discussion on the preliminary research conducted and basic understanding of the chosen topic, which is **A Study on Fatigue Behaviour of Beam Column Joint Under Low Earthquake Loading**. For this project, the structural component of beam-column joint in Malaysian standard school buildings are studied for its behaviour under seismic action. A three storey school building in Malaysia is chosen as a case study. The exterior and end joint of the school building is selected and samples of that joint are fabricated. Lab testing were conducted to investigate the properties of beam column joint when a cyclic loading is applied until it failure. The record of a 2007 Sumatra earthquake which had a magnitude of peak ground accelereation of 0.015g is obtained from Consortioum of Organizations for Strong-Motion Observation Systems (COSMOS) and used to investigate the time-history response of the school building. A commercial software, STAAD.Pro is used to analyse the response of the school building to the earthquake. Rainflow cycle counting in time domain is then examined by taking the time history of load from STAAD.Pro as the input. Number of cycles is determined from the time history. After the total number of cycles in both time and frequency domain approaches are found, Palmgren-Miner rule also known as linear damage theory, is used to estimate the fatigue life. From the study done, it is observed that the structure undergoing earthquake of 3.7 MMI experience minimal damage. The significance of this research would be important to evaluate the condition of the structure if it is able to withstand the shaking as it was not designed to perform the job.

ACKNOWLEDGEMENT

In the name of Allah, the Most Merciful, the Most Gracious. Praise to Him, who gave an opportunity to the author to complete his Final Year Project. Through Him everything is possible and this project can be completed despite those obstacles and hardship encountered.

The author would like to express his greatest gratitude to his project supervisor, Ms Nabilah Bt. Abu Bakar for her guidance and supervision. Her continuous motivation and commitment to this project has made it more meaningful and worthwhile .

Thousand of thanks to the other colleagues, Mr. Amri, Voon Chet Chie and also technicians from Civil Engineering Department, Mr. Johan, Mr. Idris, Mr. Meor, Mr. Iskandar, Mr. Zaaba and Mr. Hafiz who have given fullest support and help in finishing the project during experimental work.

Last but not least, the author would like to thank his family whom had supported and motivated him in many kinds of ways. For always being there to lift up his spirit and provide his all the needs to complete this project.

TABLE OF CONTENT

LIST OF FIGURES

LIST OF TABLES

ABBREVIATION

MMD	Malaysian Meteorological Department
S-N	Stress – No of Cycle
PWD	Public Works Department
COSMOS	Consortium of Organizations for Strong Motion Observation Systems
FDI	Fatigue Damage Index

CHAPTER 1

INTRODUCTION

1.1 BACKGROUND

The Indian Ocean earthquake, known in the scientific community as the Sumatra-Andaman earthquake on December 2004 which caused the deadly tsunami was felt in Malaysia, though at a small scale which didn't cause major damages such as collapsed buildings with casualties. But from then, the concern of whether buildings in Malaysia are able to withstand the shaking if the same magnitude of earthquake were to happen somewhere nearer to Malaysia rises.

In the analysis of reinforced concrete moment resisting frames the joints are generally assumed as rigid. In Indian practice, the joint is usually neglected for specific design with attention being restricted to provision of sufficient anchorage for beam longitudinal reinforcement. This may be acceptable when the frame is not subjected to earthquake loads. There have been many catastrophic failures reported in the past earthquakes, in particular with Turkey and Taiwan earthquakes occurred in 1999, which have been attributed to beam-column joints. The poor design practice of beam column joints is compounded by the high demand imposed by the adjoining flexural members (beams and columns) in the event of mobilizing their inelastic capacities to dissipate seismic energy. Unsafe design and detailing within the joint region jeopardizes the entire structure, even if other structural members conform to the design requirements.

Table 1.1 shows the data taken from the Malaysian Meteorological Department's (MMD) official website showing record of earthquakes in Malaysia dating back to 1909. The intensity of the recorded earthquakes, measured according to the Modified Mercalli Scale, is explained in details in **Appendix C**.

Table 1.1. Earthquakes felt in Malaysia

State	Frequencies	Maximum Intensity Observed (Modified Mercalli Scale)
Peninsular Malaysia (1909 - September 2007)		
Perlis	2	IV
Kedah	13	V
Penang	36	VI
Perak	22	VI
Selangor/Kuala Lumpur	46	VI
Negeri Sembilan	7	V
Melaka	15	V
Johor	27	VI
Pahang	7	III
Terengganu	1	IV
Kelantan	3	IV
Sabah (1923 - September 2007)		
Sabah	27	VII
Sarawak (1923 - September 2007)		
Sarawak	5	V

(Source: Malaysian Meteorological Department website)

A rough glance at the figures shows some coherence, that is several states along the west coast of Peninsular Malaysia – Selangor/Kuala Lumpur, Penang, Johor, and Perak have the highest frequencies of earthquakes. Coincidently, these are also the most developed states in the country, with a significant number of old and new buildings being built over the last decade. Despite charting a high growth in the construction of new buildings, these states are now at the highest risk during the occurrence of an earthquake.

In view of the safety of structures subjected to earthquakes, the Town and Country Planning Department and various related parties have commenced work to draft out guidelines that will ensure the future safety of buildings in Malaysia. As the study of earthquake on buildings is a relatively new field in Malaysia, continuous researches and experiments need to be conducted to assess the impacts.

Since past three decades extensive research has been carried out on studying the behaviour of joints under seismic conditions through experimental and analytical studies. Various international codes of practices have been undergoing periodic revisions to incorporate the research findings into practice.

Buildings in Malaysia are not designed to withstand seismic load as Malaysia have never experienced earthquake. Thus, a standard code for Malaysia is not available. For countries which are prone to earthquake, United States of America and Indonesia have their own set of code seismic code that is used in the design for buildings.

This study will be focused on a typical school buildings with a lightly reinforced beam column joint is referred and the beam-column joint capacity is analysed.

1.2 PROBLEM STATEMENT

The beam column joint is the crucial zone in a reinforced concrete moment resisting frame. It is subjected to large push and pull forces during severe ground shaking and its behaviour has a significant influence on the response of the structure. The assumption of joint being rigid fails to consider the effects of high shear forces developed within the joint. The shear failure is always brittle in nature which is not an acceptable structural performance especially in dynamic loading conditions.

In papers by Lowes and Altoontash (2003) and Pantelides et al. (2008), the authors found out that most post-earthquake structural collapses could be attributed to joint failure. Thus, in order to design a building to withstand earthquake loading, emphasis on its joint detailing would be very crucial. The joints of RC buildings in Malaysia are designed as lightly reinforced. Since the extend of earthquake loading in Malaysia is slightly different as compared to other countries in high-seismic zones, a more practical study on the effects of earthquake loading on a joint for the building in Malaysia should be carried out. The study should be oriented towards the Malaysian earthquake scenario.

1.3 OBJECTIVES AND SCOPE OF STUDY

The objectives of the project are as follows:

- Testing joint samples under cyclic loading until failure.
- Analysing the effects of low magnitude earthquake to the structure using STAAD.Pro.
- Calculating the fatigue damage of the equivalent cyclic response.

The scope of this study would be on the testing the joint samples and analyzing three storey school building in Malaysia using STAAD.Pro. This research is specifically meant to investigate the effects of earthquake loading on RC buildings in Malaysia which the author focusing on typical school buildings with a lightly reinforced beam column joint. The project would cover the following:

- The sample or structure analysed is a school designed by Malaysia Public Work Department (JKR)
- The project would involve testing the concrete joints under static and cyclic loading to investigate its fatigue behaviour.
- Using STAAD Pro., time-history analysis of Sumatra 2007 earthquake will be used to analyse its effect to the structure.

CHAPTER 2

LITERATURE REVIEW

2.1 Earthquake

An earthquake is a tremor of the earth's surface usually triggered by the release of underground stress along fault lines. This release causes movement in masses of rock and resulting shock waves. In spite of extensive research and sophisticated equipment, it is impossible to predict an earthquake, although experts can estimate the likelihood of an earthquake occurring in a particular region.

In 1935, American seismologist Charles Richter developed a scale that measures the magnitude of seismic waves. Called the Richter scale, it rates earth tremors on a scale from 1 to 9, with 9 being the most powerful and each number representing an increase of ten times the energy over the previous number. According to this scale, any quake that is higher than 4.5 can cause damage to stone buildings; quakes rated a magnitude of 7 and above are considered very severe. The Mercalli scale, was devised by Italian seismologist Giuseppe Mercalli to measure the severity and intensity of an earthquake in terms of its impact on a particular area and its inhabitants and buildings.

Some earthquakes are too small to be felt but can cause movement of the earth, opening up holes and displacing rocks. Shock waves from a very powerful earthquake can trigger smaller quakes hundreds of miles away from the epicenter. Approximately 1,000 earthquakes measuring 5.0 and above occur yearly. Earthquakes of the greatest intensity happen about once a year and major earthquakes (7.0-7.9) occur about 18 times a year. Strong earthquakes (6.0-6.9) occur about 10 times a month and moderate earthquakes (5.0-5.9) happen more than twice daily. Most earthquakes are not even noticed by the general public,

since they happen either under the ocean or in unpopulated areas. Sometimes an earthquake under the ocean can be so severe, it will cause a tsunami, responsible for far greater damage. The greatest danger of an earthquake comes from falling buildings and structures and flying glass, stones and other objects.

2.2 Beam-column joint

Beam-column connections in reinforced concrete (RC) frame structures under earthquake-induced lateral displacements are generally subjected to large shear stresses that may lead to significant joint damage and loss of stiffness in the structure. According to Gustavo J. Parra-Monesinos, Sean W.Peterfreund and Shih Ho Chao (2005), current design recommendations for RC beam-column joints in earthquake-resistant construction given by Joint ACI-ASCE Committee 352 (2002) focus on three main aspects: 1) confinement requirements; 2) evaluation of shear strength and 3) anchorage of beam and column bars passing through the connection. Additionally, a strong column-weak beam behavior must be ensured and frame members or regions expected to experience large reversed inelastic deformations must be properly detailed to ensure sufficient displacement capacity during earthquakes. ACI design recommendations for RC beam-column connections follow a strength-based approach, where the connection shear strength is checked against the expected force demands imposed by adjoining members. Based on those recommendations, the joint is assumed to behave satisfactorily during earthquakes if its shear strength exceeds the shear demand, a strong column-weak beam mechanism is ensured, and sufficient transverse reinforcement and anchorage length for reinforcing bars passing through the connection are provided. The minimum amount and maximum spacing of joint transverse reinforcement are based on the requirements for critical regions of RC columns, which when combined with the longitudinal reinforcement from beams and columns, often lead to severe reinforcement congestion and construction difficulties. Furthermore, the need to satisfy the anchorage length requirements

for beam and column longitudinal bars may require either the use of large column and/or beam sections or a large number of small diameter bars, which might in turn increase reinforcement congestion in the connection.

The joint is defined as the portion of the column within the depth of the deepest beam that frames into the column. In a moment resisting frame, three types of joints can be identified via interior joint, exterior joint and corner joint (Fig.2.1). When four beams frame into the vertical faces of a column, the joint is called as an interior joint. When one beam frames into a vertical face of the column and two other beams frame from perpendicular directions into the joint, then the joint is called as an exterior joint. When a beam each frames into two adjacent vertical faces of a column, then the joint is called as a corner joint. The severity of forces and demands on the performance of these joints calls for greater understanding of their seismic behaviour. These forces develop complex mechanisms involving bond and shear within the joint. The objective of the paper is to review and discuss the well postulated theories for seismic behaviour of joints in reinforced concrete moment resisting frames.

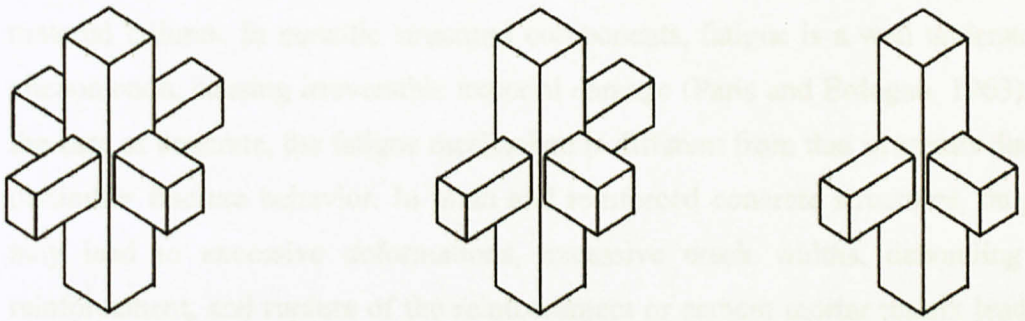

Figure 2.1. Types of Joints in a Frame

2.3 Fatigue

In recent years, condition monitoring, repair, and retrofitting of existing structures such as buildings and bridges have been among the most important challenges in civil engineering. The primary reasons for condition assessment and consequent maintenance/strengthening of structures include enhancement of resistance to withstand underestimated loads, increase in the load-carrying capacity for higher permit loads, restoration of lost carrying capacity due to corrosion of structural steel or reinforcing bars, and cracking of concrete or other types of degradation caused by aging. Whereas a lot of research has been done in the area of repair and retrofitting of aged structures, not much has been reported on the assessment of current structural condition so as to estimate the residual capacity at present-day enhanced load levels. The assessment requires that any damage in the structure be detected before it has developed to a dangerous size. The concepts of fracture mechanics may be used as a mathematical tool for assessment of residual strength for providing equations that can be used to determine how cracks grow and how cracks affect the fracture strength of a structure.

It is well known to designers that fatigue accounts for a majority of material failures. In metallic structural components, fatigue is a well understood phenomenon, causing irreversible material damage (Paris and Erdogan, 1963). In the case of concrete, the fatigue mechanism is different from that in metals due to dissimilar fracture behavior. In plain and reinforced concrete structures, fatigue may lead to excessive deformations, excessive crack widths, debonding of reinforcement, and rupture of the reinforcement or cement mortar matrix leading to structural collapse (Perdikaris and Calomino, 1987).

Fracture of concrete is characterized by the presence of a fracture process zone (FPZ) at the crack tip. The effective crack length is longer than the true crack but shorter than the true crack plus the FPZ. The FPZ is a zone where the cement mortar matrix is intensively cracked. Along the FPZ, there is a discontinuity in displacements but not in the stresses. The stresses are themselves a function of the crack opening displacement (COD). At the tip of the FPZ, tensile stress is equal to tensile strength of the material and it gradually reduces to zero at the tip of the true crack. It is assumed that under low-cycle fatigue loading, the resulting damage, that is, the decrease in load-carrying capacity and stiffness, occurs primarily in the FPZ and not in the undamaged material (Foreman et al, 1967). In most of the nonlinear material models for fatigue of concrete, it is assumed that only the FPZ is responsible for the variation of material properties during cyclic loading. If the fracture process zone exhibits greater sensitivity to fatigue loading than the surrounding material, then the fatigue behavior can be considered to be dependent on loading history (Slowik et al, 1996). Furthermore, the size, shape, and fatigue behavior of the FPZ are dependent on specimen size and geometry (Zhang et al, 2001). Thus, loading history is of paramount importance in fatigue behavior of concrete and only a nonlinear fracture mechanics model can rigorously explain it. A method for residual life prediction of plain concrete has been proposed by Zhang and Wu (1997), but it is based on the S - N curve approach, where S is the cyclic stress level and N is the number of cycles to failure.

2.4 Rainflow Counting Method

Counting methods have initially been developed for the study of fatigue damage generated in aeronautical structures. Since different results have been obtained from different methods, errors could be taken in the calculations for some of them. Level crossing counting, peak counting, simple range counting and rainflow counting are the methods which are using stress or deformation ranges. One of the preferred methods is the rainflow counting method. Rainflow cycle counting method has initially been proposed by M.Matsuiski and T.Endo to count the cycles or the half cycles of strain-time signals. Counting is carried out on the basis of the stress-strain behavior of the material. This is illustrated in Figure 2.2 as the material deforms from point a to b, it follows a path described by the cyclic stress-strain curve. At point b, the load is reversed and the material elastically unloads to point c. When the load is reapplied from c to d, the material elastically deforms to point b, where the material remembers its prior history, i.e. from a to b, and deformation continues along path a to d as if event b-c never occurred.

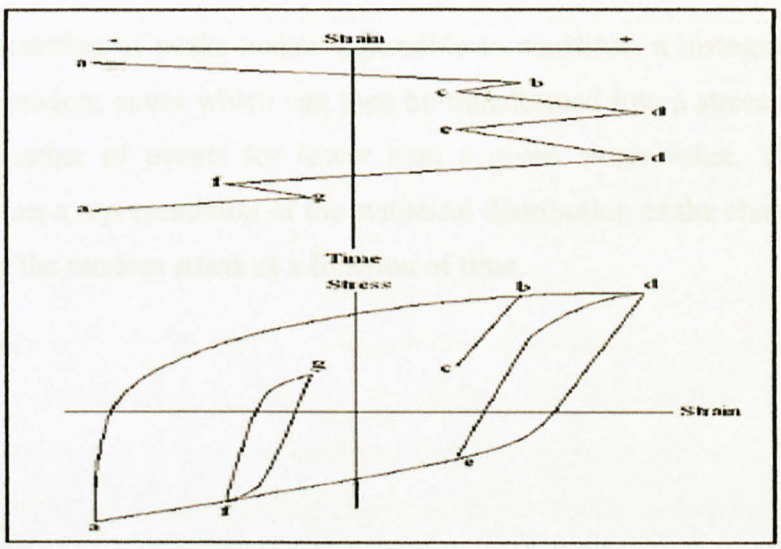

Figure 2.2. Stress – strain cycles

The signal measured, in general, a random stress S(t) is not only made up of a peak alone between two passages by zero, but also several peaks appear, which makes difficult the determination of the number of cycles absorbed by the structure. An example for the random stress data is shown in Figure 2.3.

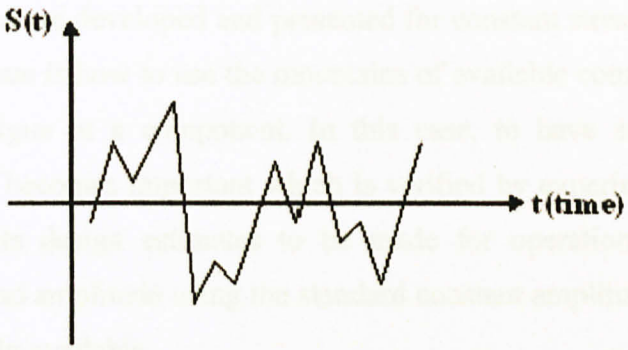

Figure 2.3. Random stress Fluctuation

The counting of peaks makes it possible to constitute a histogram of the peaks of the random stress which can then be transformed into a stress spectrum giving the number of events for lower than a given stress value. The stress spectrum is thus a representation of the statistical distribution of the characteristic amplitudes of the random stress as a function of time.

2.5 Palmgren – Miner Rule

Almost all available fatigue data for design purposes is based on constant amplitude tests. However, in practice, the alternating stress amplitude may be expected to vary or change in some way during the service life when the fatigue failure is considered. The variations and changes in load amplitude, often referred to as spectrum loading, make the direct use of S-N curves inapplicable because these curves are developed and presented for constant stress amplitude operation. The key issue is how to use the mountains of available constant amplitude data to predict fatigue in a component. In this case, to have an available theory or hypothesis becomes important which is verified by experimental observations. It also permits design estimates to be made for operation under conditions of variable load amplitude using the standard constant amplitude S-N curves that are more readily available.

Many different cumulative damage theories have been proposed for the purposes of assessing fatigue damage caused by operation at any given stress level and the addition of damage increments to properly predict failure under conditions of spectrum loading. Collins, in 1981, provides a comprehensive review of the models that have been proposed to predict fatigue life in components subject to variable amplitude stress using constant amplitude data to define fatigue strength. The original model, a linear damage rule, originally suggested by Palmgren (1924) and later developed by Miner (1945). This linear theory, which is still widely used, is referred to as the Palmgren-Miner rule or the linear damage rule. Life estimates may be made by employing Palmgren-Miner rule along with a cycle counting procedure. Target is to estimate how many of the blocks can be applied before failure occurs. This theory may be described using the S-N plot.

In this rule, the assumptions can be summarized as follows:

i) The stress process can be described by stress cycles and that a spectrum of amplitudes of stress cycles can be defined. Such a spectrum will lose any information on the applied sequence of stress cycles that may be important in some cases.

ii) A constant amplitude S-N curve is available, and this curve is compatible with the definition of stress; that is, at this point there is no explicit consideration of the possibility of mean stress.

The constant amplitude S-N curve is shown in Figure 2.4. By using the S-N data, number of cycles of S_1 is found as N_1 which would cause failure if no other stresses were present. Operation at stress amplitude S_1 for a number of cycles n_1 smaller than N_1 produces a smaller fraction of damage which can be termed as D_1 and called as the damage fraction.

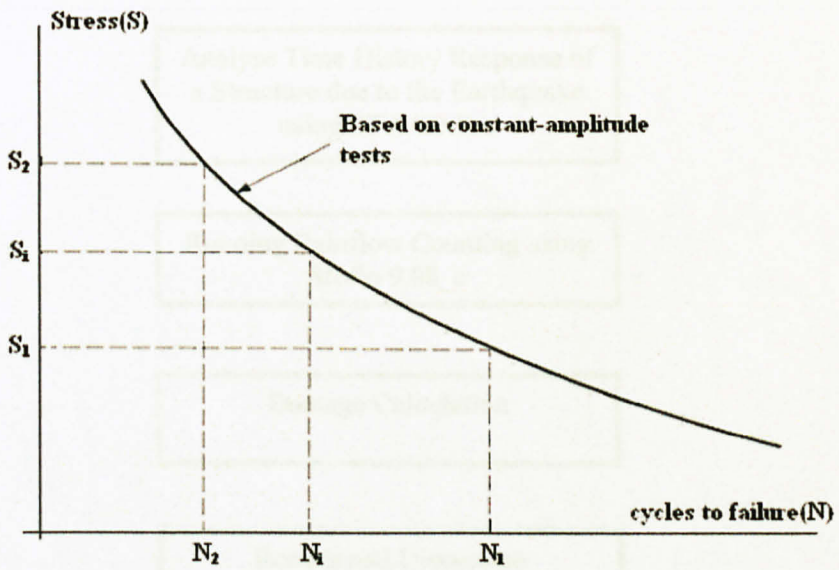

Figure 2.4 : Constant Amplitude of S-N Curve

CHAPTER 3 : METHODOLOGY

The project will be conducted as accordance to the flow chart shown in Figure 3.1.

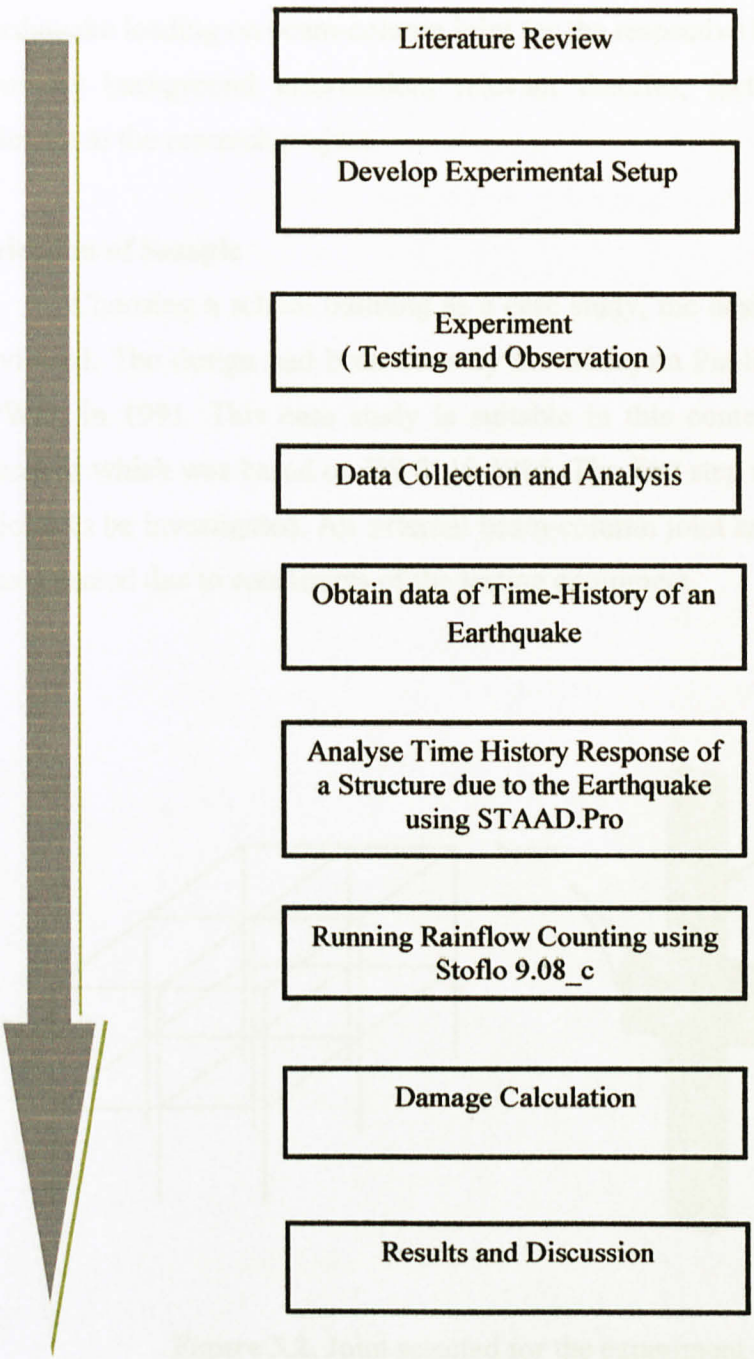

Figure 3.1. Flow Chart of Project Methodology

3.1 Literature Review

During the early stage of the project, literature review is completed to acquire background knowledge about current RC buildings in Malaysia. Literature review is done on written materials subjected to the effect of earthquake loading on beam-column joint for the respective buildings. The review provides background information, relevant theories, facts and data that are relevant to the research project.

3.2 Selection of Sample

Choosing a school building as a case study, the design of the structure is reviewed. The design had been done by the Malaysia Public Works Department (PWD) in 1991. This case study is suitable in this context due to the design standard which was based on BS 8110:1985. The first step required was to select a joint to be investigated. An external beam-column joint as shown in Figure 3.2 was selected due to constraints of the testing equipment.

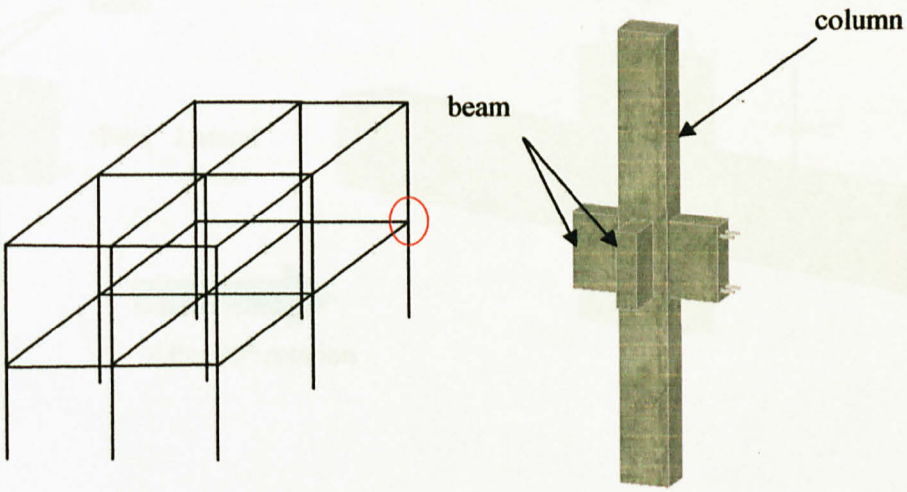

Figure 3.2. Joint selected for the experiment

During an earthquake, a building is subjected to ground acceleration, thus inducing lateral forces on the structure. In order to simulate the earthquake lateral force acting on the joint, the sample needs to be reoriented. Figure 3.3 shows the proposed orientation of the joint sample to be tested.

The selected joint is rotated 90° for several reasons:-

- The apparatus is only limited to applying force in the vertical direction. There are no other apparatuses available in-house to simulate the horizontal force.

- No specific mounting frame was fabricated in order hold the column in its actual position. It was more economical to utilize available apparatuses and fabricate lesser new ones.

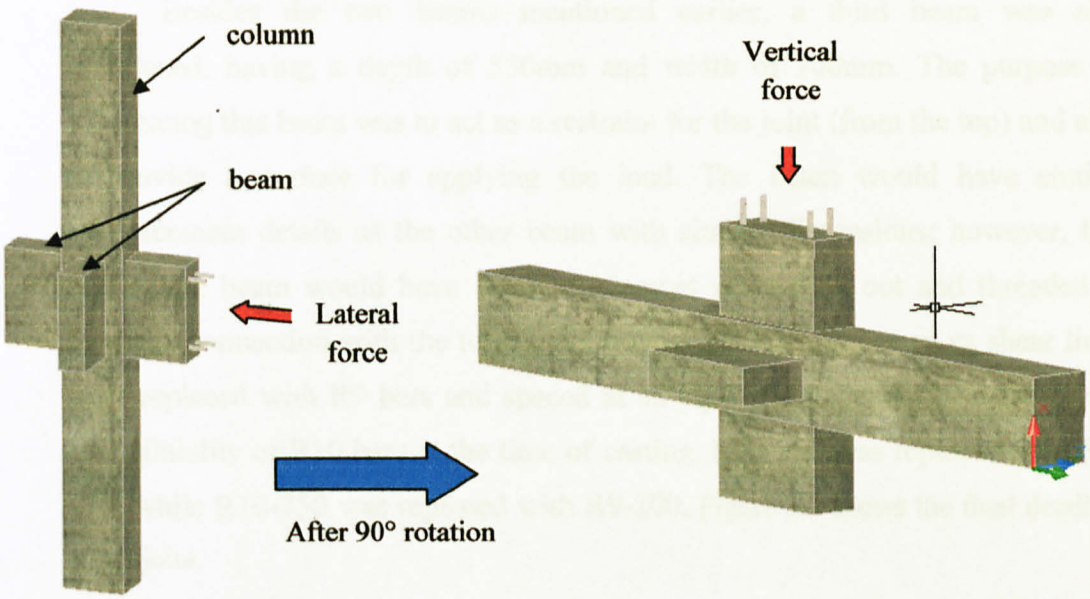

Figure 3.3. Proposed orientation of the beam-column joint for testing.

Having selected the joint, the detailing of reinforcement bars and dimensions were determined based on the structural drawings by PWD. The length of column was fixed at 3250mm, taking the vertical distance from the middle of one floor to the floor above. The column had a cross section of 350mm depth and 250mm width. The main reinforcement bars for the column were 4-Y20, with shear links of R10-200.

There are two different sizes of beam in this joint. The beam parallel to the direction of the applied force had a depth of 550mm and a width of 200mm. The top and bottom reinforcement bars used were 2-Y20 respectively, with shear links of R10-200. The beam perpendicular to the direction of the applied force had a depth of 550mm and a width of 150mm. The top and bottom reinforcement bars were 2-Y16 respectively, with shear links of R10-250.

Besides the two beams mentioned earlier, a third beam was also introduced, having a depth of 550mm and width of 200mm. The purpose of introducing this beam was to act as a restraint for the joint (from the top) and also to provide a surface for applying the load. The beam would have similar reinforcement details as the other beam with similar dimensions; however, this end of the beam would have its reinforcement protruding out and threaded to facilitate connection with the testing apparatus. All R10 bars used as shear links were replaced with R9 bars and spaced at an equivalent spacing because of the unavailability of R10 bars at the time of casting. R10-200 was replaced with R9-175, while R10-250 was replaced with R9-200. Figure 3.4 shows the final detailing of the joint.

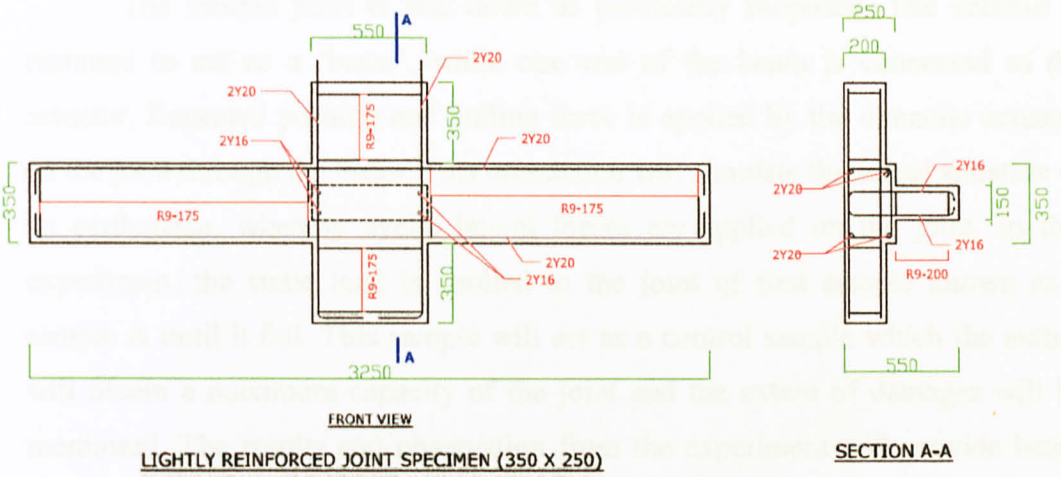

Figure 3.4. Details of the Joint

3.3 Experimental Setup

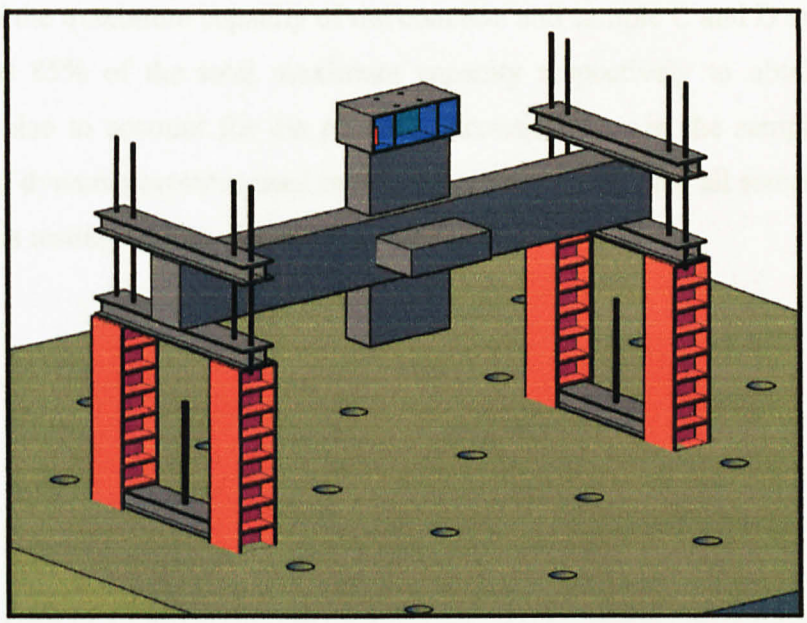

Figure 3.5. Experimental setup for the proposed beam column joint sample

The sample joint is laid down as previously proposed. The column is assumed to act as a 'beam', while one end of the beam is connected to the actuator. Repeated pushing and pulling force is applied by the dynamic actuator on the joint through the beam. This orientation will simulate the actual situation of an earthquake, whereby cyclic lateral forces are applied on the joint. In this experiment, the static load is applied to the joint of first sample known as a sample A until it fail. This sample will act as a control sample which the author will obtain a maximum capacity of the joint and the extent of damages will be monitored. The results and observation from the experiment will provide better understanding on the behaviour of the lightly reinforced concrete joint. The crack patterns are monitored throughout the experiment and the strain and deflection datas are collected from the computer. The experiment is repeated on 3 additional samples known as sample B, C and D by using cyclic loading until it fails with the limitation of 150,000 cycles per sample. Sample B will be tested based on 20% load of the maximum capacity of the concrete and sample C and D are based on 60% and 85% of the total maximum capacity respectively to obtain more results and also to account for the possible inconsistencies in the samples. The frequency of dynamic actuator used in this experiment is 5Hz for all samples. The results of this testing will be discussed at chapter 4.

The experiment involves the use of a dynamic actuator with a capacity of 2000kN, mounted on a universal frame (Refer to Figure 3.6).

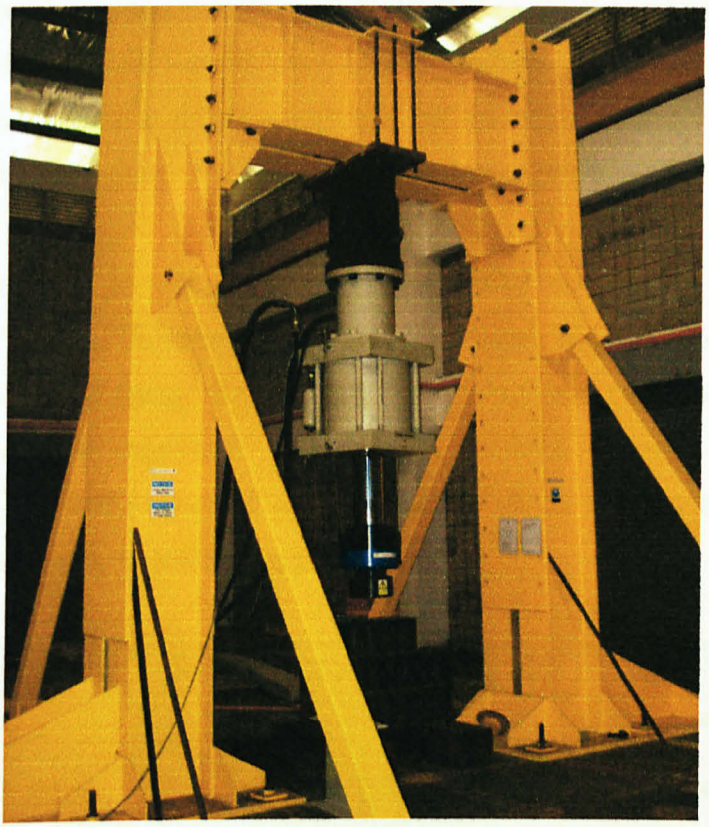

Figure 3.6. Dynamic actuator mounted on a universal frame

The universal frame is fixed onto a strong floor, with voids at every 1 m interval. These voids in the floor will be utilized to secure the support system for the joint sample onto the ground as shown in Figure 3.6. The sample of the beam-column joint is then secured down to the supports by means of bolts and plate girders to prevent it from movement. Stiffened plate girders are used as the supports, supporting the sample at 2 points. The design of the support system, including connection details are done in accordance to BS 5950: Structural use of steelwork in building.

3.4 Data of Time-History for Sumatra 2007 Earthquake

In analyzing the-time history response, a sample of an earthquake data was obtained from the consortium of organizations for strong Motion Observation Systems (COSMOS) Virtual Data Center Website. COSMOS is a non-profit organization aimed to create awareness for earthquake safety. It provides free acquisition and application of strong-motion data to users.

The time history data of an earthquake occurred in the Kepulauan Mentawai Region, Indonesia is chosen. The region located about 185 km (115 miles) SSE of Padang, Sumatra or about 755 km (470 miles) WNW of JAKARTA. The magnitude 8.4 and 7.8 southern Sumatra earthquakes of September 12, 2007 occurred as the result of thrust faulting on the boundary between the Australia and Sunda plates.

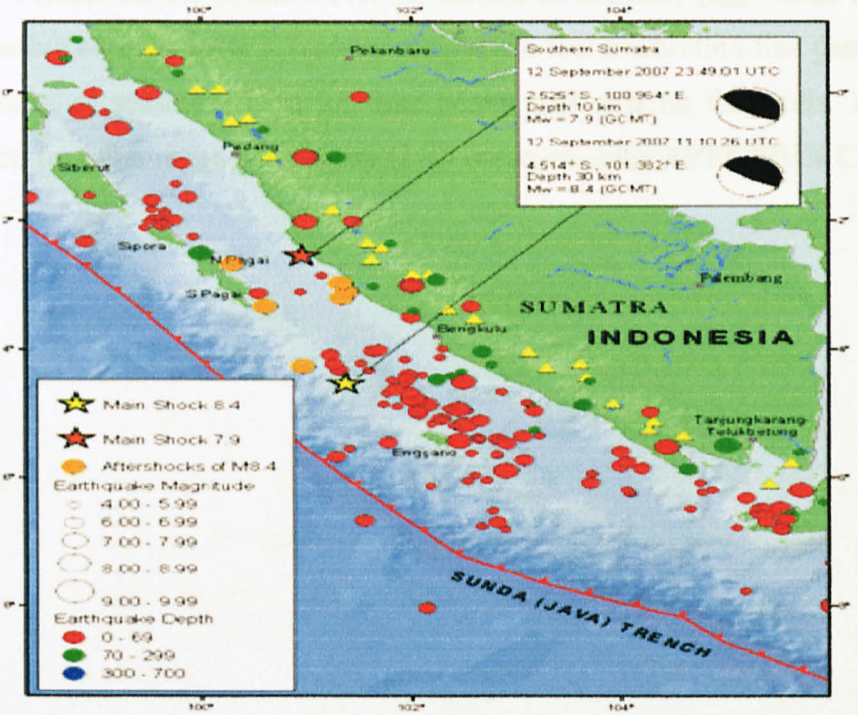

Figure 3.7. Location of Earthquake occurred at Pulau Sumatra (2007)

An analysis of acceleration and intensity correlations has been carried out using a new, worldwide data sample compiled for this study from data measured from nearly 1500 strong-motion accelerograms. This new data sample has been extensively analyzed using a variety of statistical models. It has been found that the correlation equation relating peak horizontal ground acceleration (a_H) to Modified Mercalli intensity (I_{mm}) which best describes the trends in the subset of this new sample consisting of the nearly 900 observations for which $a_H \geq 10$ cm/sec^2 (J.R. Murphy and L. J. O'Brien, Bulletin of the Seismological Society of America. Vol. 67, No.3, pp. 877-915, June 1977) is : -

$$\textbf{Log } a_H = 0.25\, I_{mm} + 0.25 \text{ .....equation 3.1}$$

Thus, for the data obtained from COSMOS for Kepulauan Mentawai (2007), the peak ground acceleration (a_H) for that particular earthquake is 15cm/sec^2. Based on the equation 3.1, the calculated intensity (I_{mm}) value for that corresponding earthquake is 3.7 where people can feel a vibration like passing of heavy trucks or sensation of a jolt like heavy ball striking the walls. Further description for other range of intensity (I_{mm}) is shown at the **APPENDIX C**.

3.5 Analysis of Time-History Response of Structure

Using the Time-History data of 2007 Sumatra earthquake, the school structure is modelled in STAAD.Pro and the seismic load is imposed on the structure. The results of the analysis are reported in Chapter 4.

3.6 Rainflow Counting Method

The rainflow-counting algorithm also known as the "rain-flow counting method" is used in the analysis of fatigue data in order to reduce a spectrum of varying stress into a set of simple stress reversals. Its importance is that it allows the application of Miner's rule in order to assess the fatigue life of a structure subject to complex loading. The author has used StoFlo 9.08_c software in order to calculate the total amount of cycles for a various ranges of stress. The stress of the samples is actually calculated based on the results of time history graph from the STAAD.Pro. StoFlo 9.08_c is a free software application within Microsoft Excel. It contains code that will perform rainflow cycle counting. The required input is ASCII data. The output is the range and mean of each cycle. The result of this method is shown at Chapter 4.

3.7 Damage Calculation (Palmgren-Miner Rule)

Calculation of damage due to repeated cyclic loads is a well established methodology in some fields of engineering. With the data from seismic loads which is not made up of complete and consistent cycles, then the Palmgren-Miner Rule (Miner,1945) is used to predict the damaged per cycle as

$$D_i = 1/N_{fi}$$

Where D is the damage for cycles of magnitude i and N is the number of cycles to failure at level i. The total damage to a member over the complete cycling history is then estimated as

$$\mathbf{FDI = N_i/N_{fi}}$$

Where FDI is the fatigue damage index, or total damage to the element due to cyclic load, n is the number of different cycle amplitudes in the loading history, and N_i, is the number of cycles at amplitude i. Values of FDI greater than or equal to 1.0 indicate a low-cycle fatigue fracture of the member.

CHAPTER 4

RESULT AND DISCUSSION

4.1 Cube Test Results

The cubes are having concrete grade of 30. Compressive tests have been carried out on the three cube samples for 8, 14 and 28 days strength respectively. Figure 4.1 shows that the stress of cubes samples increase as the days increase.

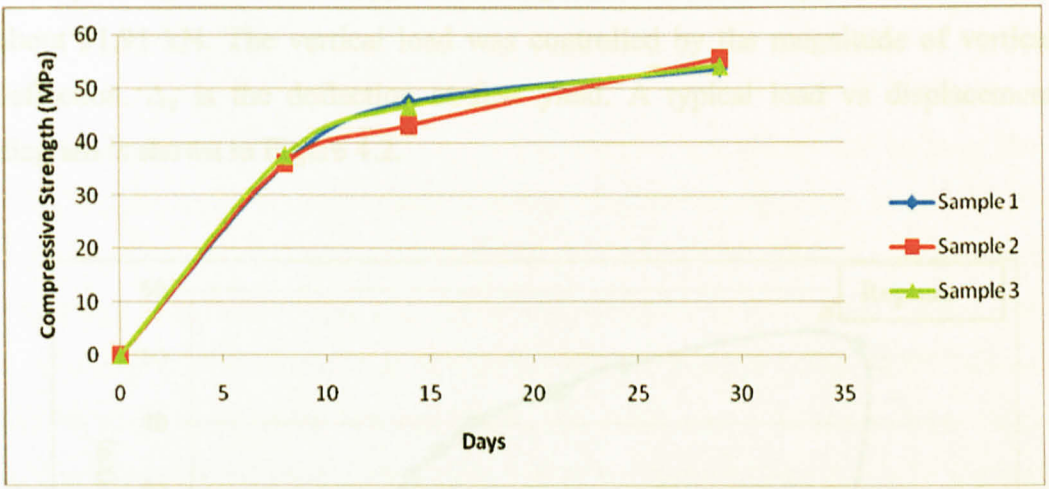

Figure 4.1. Cubes Compressive Strength vs Days

From the graph, it can be seen that the concrete strength exceeds the design strength of 30N/mm2. This may be due to the type of cement being used in the concreting process, which may have contained admixtures that would enhance the concrete strength.

4.2 Static Load Test

In this test, a vertical static load was applied to the connecting beam column stage by stage until failure of the sample occurred. This applied load which was specified 0.2 kN per second is constantly increased throughout the test until the sample fail. Failure was indicated by a marked increase in beam deflection accompanied by rapid decrease in the vertical load. The strength of the beam column joint samples is indicated by the ultimate load, ρ_u. The value of corresponding ultimate load, ρ_u of the sample is listed in the **Appendix B** which is about 51.91 kN. The vertical load was controlled by the magnitude of vertical deflection. Δ_y is the deflection at first yield. A typical load vs displacement diagram is shown in Figure 4.2.

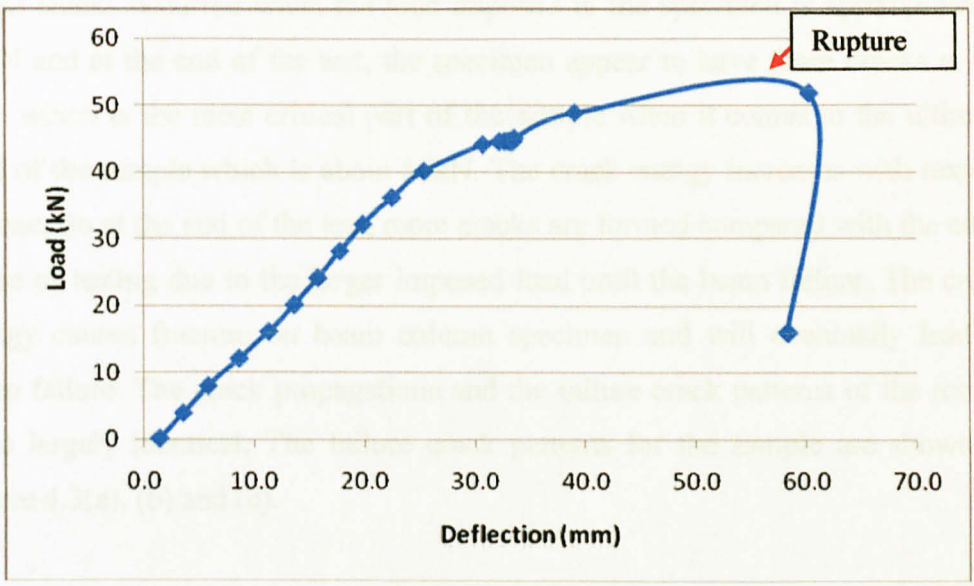

Figure 4.2. Load (kN) vs Displacement (mm) Diagram

4.3 Cyclic Load test

In this test, a push and pull forces was applied to the connecting beam column joint stage by stage until failure of the sample occurred. This applied load was limited to 150,000 cycles per sample which the frequency of the dynamic actuator was specified 5Hz for the samples. The sample showed no failure after 20kN of cyclic load was applied. This indicates that the low magnitude of load gives zero damage to the structure.

4.4 Cracking Behaviour

Generally, the beam column joint samples are all appear to have their initial cracks due to improper casting, conducting and transporting. In this test, the initial cracks occurred when the load imposed to the specimen is approximately 44kN and at the end of the test, the specimen appear to have more cracks at the joint which is the most critical part of the sample when it comes to the ultimate load of the sample which is about 50kN. The crack energy increases with respect to time. So at the end of the test, more cracks are formed compared with the early phase of testing due to the larger imposed load until the beam failure. The crack energy causes fracture on beam column specimen and will eventually lead to beam failure. The crack propagations and the failure crack patterns of the model were largely identical. The failure crack patterns for the sample are shown in Figure 4.3(a), (b) and (c).

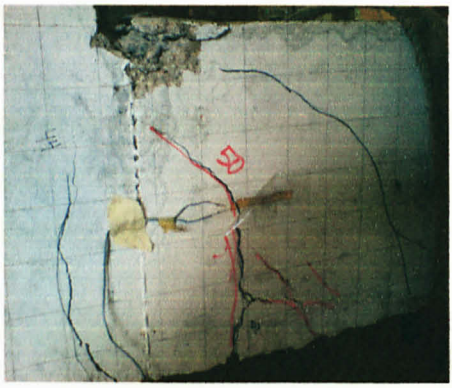

Figure 4.3(a). Cracking pattern of the sample under 50kN imposed load

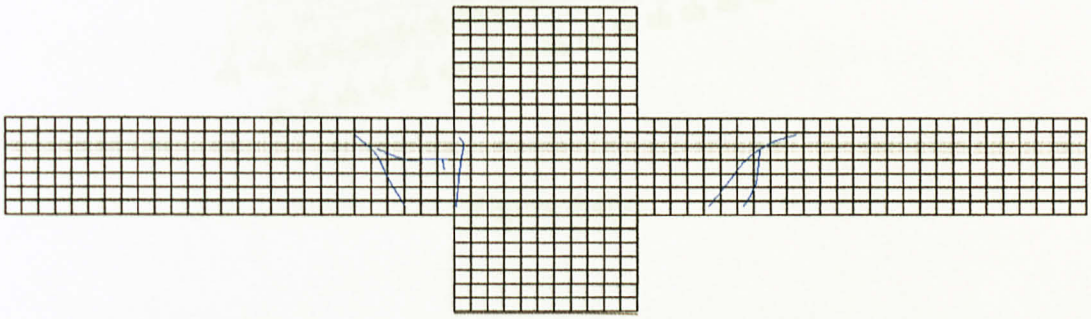

Figure 4.3(b). Cracking pattern of the sample under 44kN imposed load

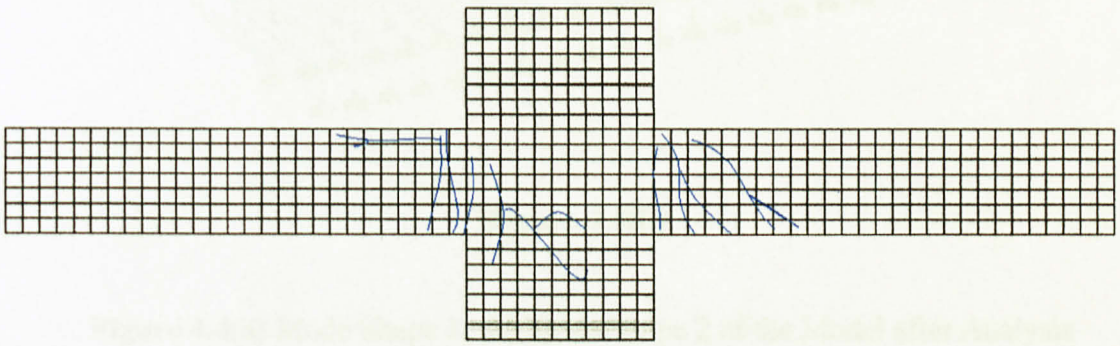

Figure 4.3(c). Overall cracking pattern of the sample during the test

4.5 Time History Response of Structure to Earthquake

The natural period of the structure is 0.691, as obtained from STAAD.Pro. Figure 4.4 shows the structure's various mode shapes. Mode shape 1 gives the response only in Z-direction, while mode shape 2 in X-direction.

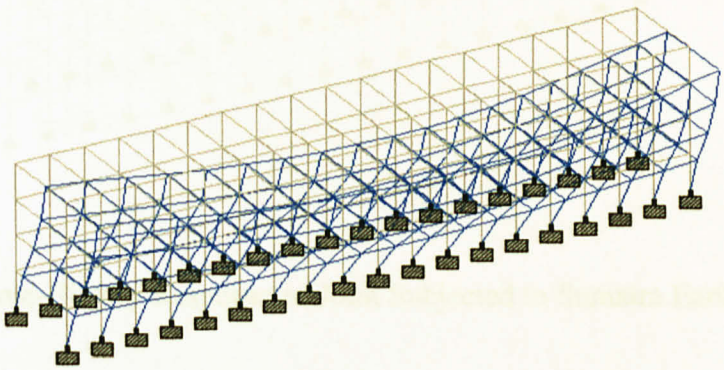

Figure 4.4(a)

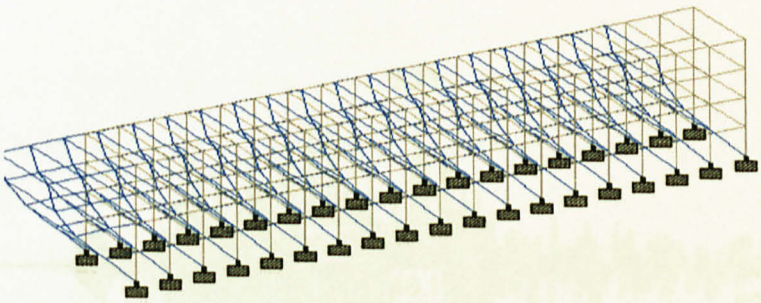

Figure 4.4(b)

Figure 4.4(a) Mode Shape 1, **(b)** Mode Shape 2 of the Model after Analysis

Node 171 was selected to obtain its time-history response.

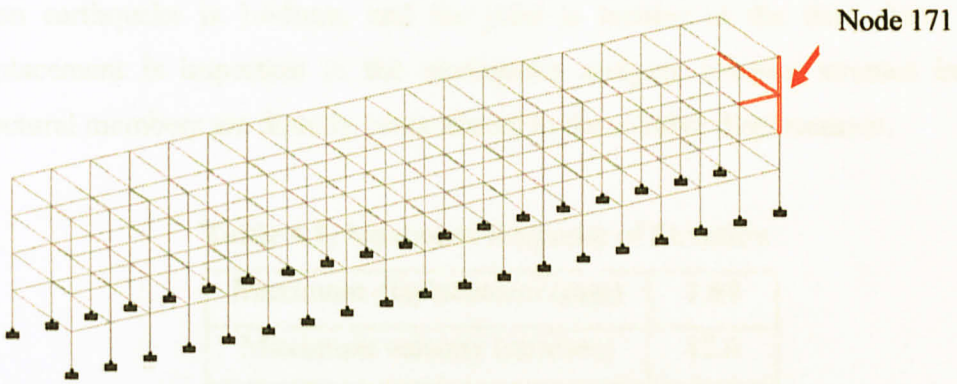

Figure 4.5. Time-History Response of Joint Subjected to Sumatra Earthquake

Figure 4.6 shows the time-history response of the node 171 as obtained from STAAD.Pro for displacement in Z-direction.

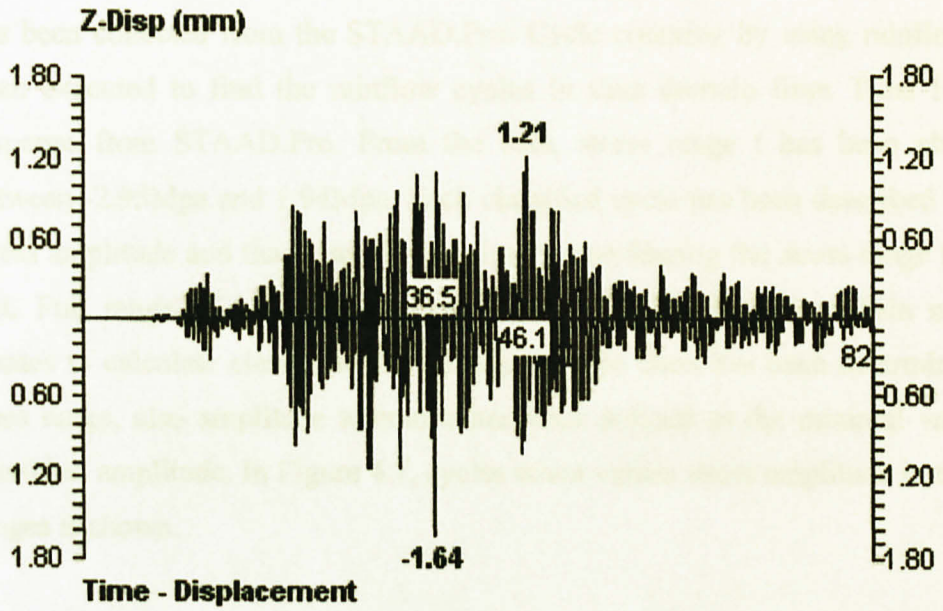

Figure 4.6 . Time-History Response (displacement) of the node 171

The maximum responses for the earthquake specified (Sumatra, 2007) are summarized in Table 4.1. The maximum displacement of the structure under the given earthquake is 1.64mm, and the joint is located at the third floor. The displacement is important in the earthquake analysis because stresses in the structural members are directly proportional to the relative displacement.

Table 4.1. Maximum Response of Structure

Maximum displacement (mm)	1.64
Maximum velocity (mm/sec)	12.4
Maximum acceleration (m/sec^2)	0.19

4.6 Rainflow Counting Method

StoFlo 9.08_c software has been used for processing the random stresses. Each random signal has been divided into the single cycles. The strain-time data has been collected from the STAAD.Pro. Cycle counting by using rainflow has been executed to find the rainflow cycles in time domain from Time History response from STAAD.Pro. From the data, stress range t has been obtained between -2.95Mpa and 1.94Mpa. Each classified cycle has been described by the stress amplitude and the mean stress value by considering the stress range for the test. Full range of possible amplitudes has been divided into certain number classes to calculate classes count. Each amplitude class has been determined by class range, also amplitude tolerance has been defined as the minimal value of classified amplitude. In Figure 4.7, cycles count versus stress amplitude in the full ranges is shown.

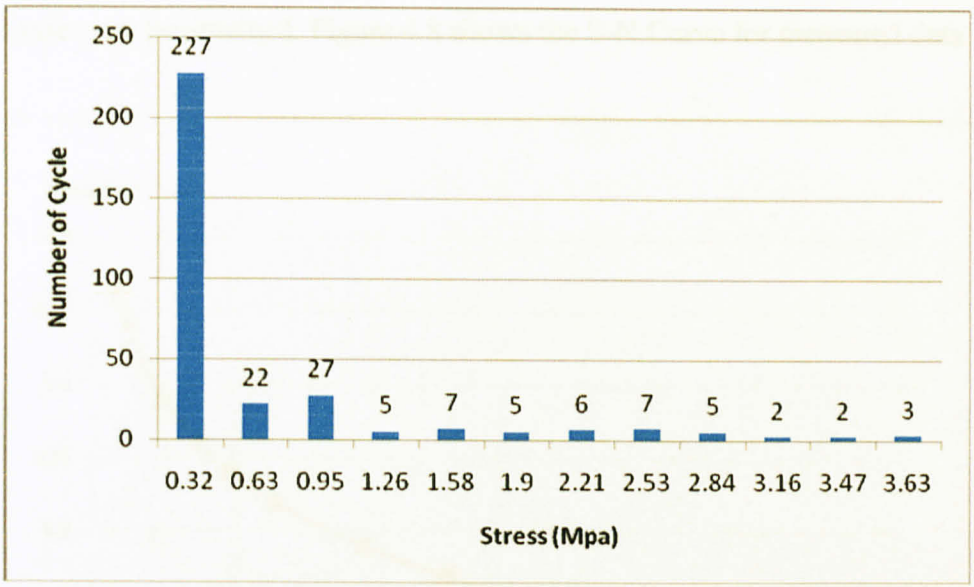

Figure 4.7 Cycle Counting in Full Range of Stress by Rainflow Method

4.7 Palmgrem – Miner Rule (Damage Calculation)

Palmgren-Miner rule also known as linear damage rule, has been applied to find the fatigue damage of the test specimen which is accepted for the Stress-Life method. Fatigue life calculation has been done by using Palmgren-Miner rule along with a cycle counting procedure.

The equation of stress versus no of cycles is obtained from research by (Binsheng Zhang & Keru Wu, Residual fatigue strength and stiffness of ordinary concrete under bending, Cement and concrete research, vol 27, No 1, pp 115-126, 1997 (2006)) as follows : -

$$S_{max}/f_c = C_F [\, 1- (1-R') B \log N \,] \text{ .....equation 4.1}$$

By putting the value of $stress_{max}$ / F_c data into Equation 4.1, the number of cycles can be obtained. Figure 4.8 shows the S-N Curve for measured data.

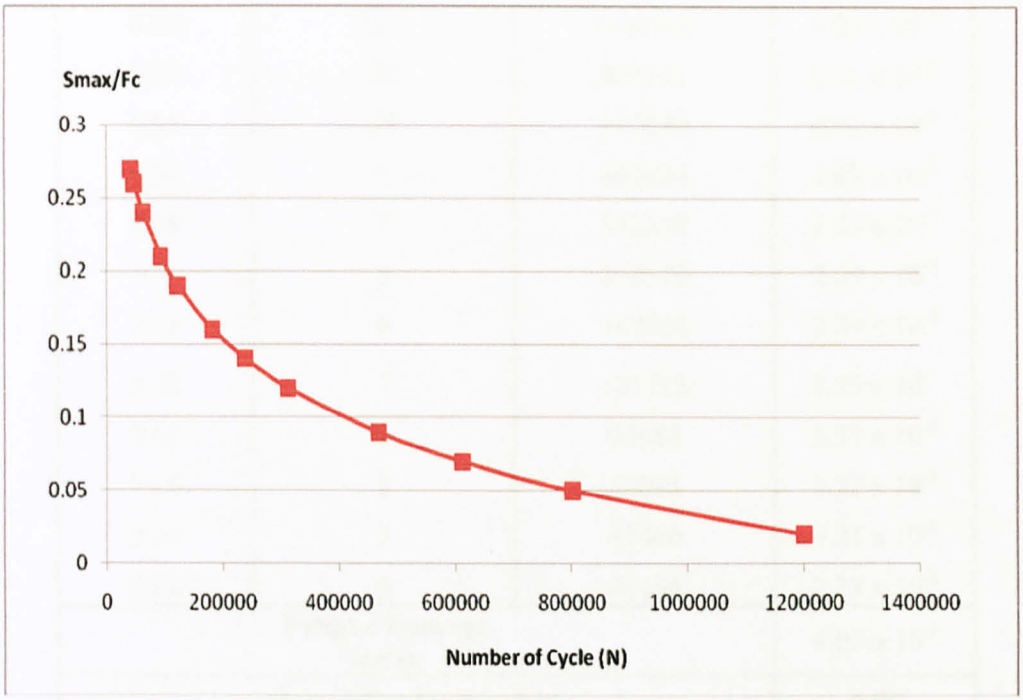

Figure 4.8. S-N Curve for Measured Data

Total damage has been calculated by dividing the number of cycles found in the time domain for each stresses to the number of cycles found from the Equation 4.1. The Fatigue Damage Index (FDI) calculation is shown in Table 4.2.

Table 4.2. Fatigue Damage Index Calculation for Measured Earthquake Data

S_{max}/F_c (Mpa)	No of cycle, N_i	No of cycles to Failure, N_{fi}	Damage , N_i/N_{fi}
0.32	227	1199743	1.89×10^{-4}
0.63	22	801162	2.75×10^{-5}
0.95	27	612080	4.41×10^{-5}
1.26	5	467624	1.07×10^{-5}
1.58	7	312269	2.24×10^{-5}
1.9	5	238570	2.09×10^{-5}
2.21	6	182266	3.29×10^{-5}
2.53	7	121713	5.75×10^{-5}
2.84	5	92988	5.37×10^{-5}
3.16	2	62095	3.22×10^{-5}
3.47	2	47440	4.21×10^{-5}
3.63	3	41466	7.23×10^{-5}
Fatigue Damage Index			6.05×10^{-4}
Remaining Fatigue Life			0.99

That is, total damage obtained from the time domain analysis:

FDI = 6.05×10^{-4}

And the remaining fatigue life = 99%

CHAPTER 5

CONCLUSION AND RECOMMENDATIONS

The strength of a beam column joint sample is experimentally determined through the test. The relationship between cracking pattern, deflection, strain ratio and failure modes are critically analyzed to study the influence of varying cyclic load ranges used to test the sample afterwards. Based on the results presented in this project, it can be concluded that:

1. The ultimate load applied to the sample which represents the strength of the beam column joint sample is 50kN.
2. The cracks appeared mostly around the critical point as expected which is the beam column connection with the increase in load imposed to the specimen.
3. Beam column sample showed no sign of failure after a 150,000 cycles of 20kN cyclic loading was applied.

From the theoretical output, it can be summarized that:

1. The maximum joint displacement that can occur is 1.64mm. This value is a linear indication of the stresses that can occur in the structural members.
2. The results of a rainflow analysis on a time history response from STAAD.Pro were successfully captured.
3. The total damage obtained from time domain analysis is almost zero which means there were apparently no damage occurred for this small earthquake amplitude.
4. The remaining fatigue life is about 99% which means the structure will be last for a long period of time.

There are many suggested future works that can be done such as:

1. All the laboratory equipments should be well-kept and maintenance must be done periodically to ensure that experiments can be done safely and on schedule
2. The materials that external suppliers provided for the laboratory should be checked regularly to make sure that they comply with the standards.

REFERENCES

Eligehausen, R., Popov, E.P. and Bertero, V.V.(1983), Local Bond Stress-slip Relationships of Deformed Bars under Generalised Excitations, *Report UCB/EERC-3/19, Earthquake Engineering Research Center*, University of California, Berkeley, 178p.

Elwood, K.J. & Moehle, J.P. (2008) Dynamic Shear and Axial-Load Failure of Reinforced Concrete Columns. *Journal of Structural Engineering*, 134 (7), 1189-1198.

Leon, R.T.(1990), Shear Strength and Hysteretic Behaviour of Beam-Column Joints, *ACI Structural Journal*, V.87, No.1, Jan-Feb, pp. 3-11

Lowes, L.N. & Altoontash, A. (2003) Modeling Reinforced-Concrete Beam-Column Joints Subjected to Cyclic Loading. *Journal of Structural Engineering,* 129 (12), 1686-1697.

MacGregor, J.G. (1988), *Reinforced Concrete Mechanics and Design*, Prentice Hall Inc.

Mayfield, B., Kong, K.F. and Bennison (1971), A. Corner joint details in structural light weight concrete, *Journal of American Concrete Institute*, Vol. 65, No.5, pp. 366-372.

Megawati, K. et al. (2005) Response spectral attenuation relationships for Sumatran-subduction earthquakes and the seismic hazard implications to Singapore and Kuala Lumpur. *Soil Dynamics and Earthquake Engineering*, 25, 11-25.

Mosley, W.H. et al. (1999) Reinforced Concrete Design: Fifth Edition. Houndmills. Palgrave.

Nilson, I.H.E., Losberg (1976), R. Reinforced concrete corners and joints subjected to bending moment, *Journal of Structural Division*, ASCE, Vol.102, No.ST6, pp.1229-1253.

Pantelides, C.P. et al. (2008) Seismic Rehabilitation of Reinforced Concrete Frame Interior Beam-Column Joints with FRP Composites. *Journal of Composites for Construction,* 12 (4), 435-445.

Park, R., and Paulay, T.(1975), *Reinforced Concrete Structures*, John Wiley and Sons, 786p.

Shiohara, H.(2001), New model for shear failure of RC interior beam-column connections, *Journal of Structural Engineering Division, ASCE, V. 127*, pp. 152-160.

Subramaniam, N., and Prakash Rao (2003), D.S. Seismic Design of Joints in RC Strucutres, *The Indian Concrete Journal*, Vol.77, No.2, pp. 883-892.

Tatsuo, O. (ed) (1997) *Dynamic Analysis and Earthquake Resistant Design*. Strong Motion and Dynamic Properties Volume 1. Rotterdam, A.A. Balkema Publishers.

Walraven, J. (1994) Rough Cracks Subjected to Earthquake Loading. Journal of Structural Engineering, 120 (5), 1510-1524.

Watson, S. and Park, R. (1994) Simulated Seismic Load Tests on Reinforced Concrete Columns. Journal of Structural Engineering, 120 (6)

APPENDICES

Appendix A

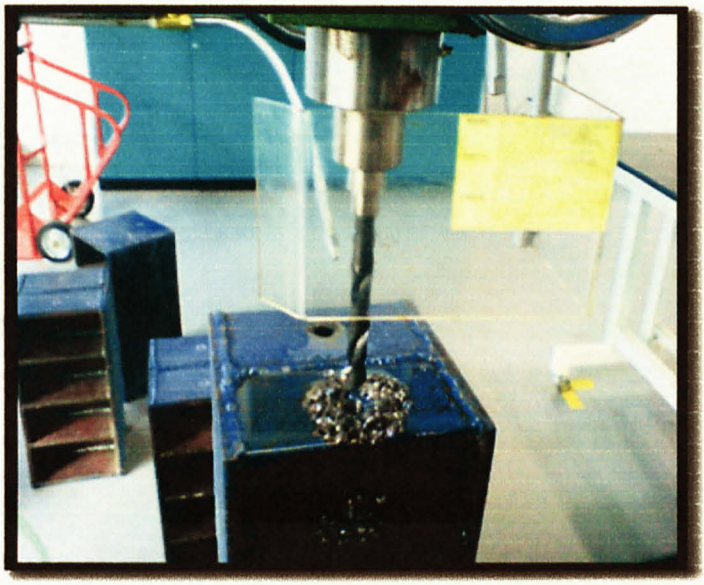

Fabricating the support system at mechanical engineering lab

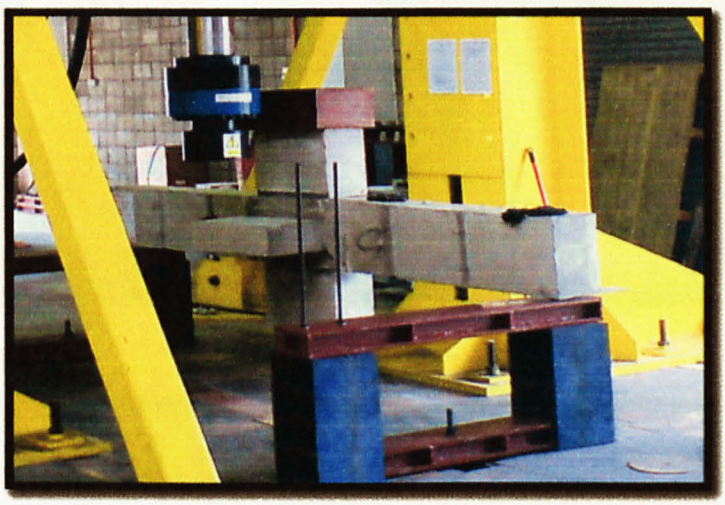

Lifting and positioning of sample and support systems

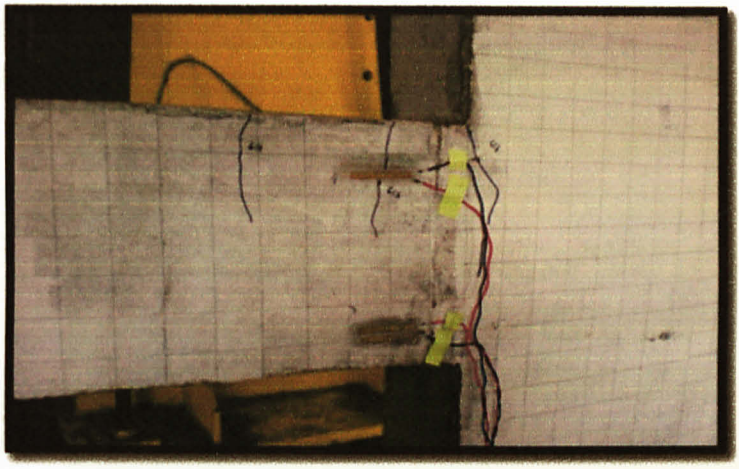

Drawing of gridlines and fixing off strain gauges

Setting up a camcorder to monitor the runnning experiment

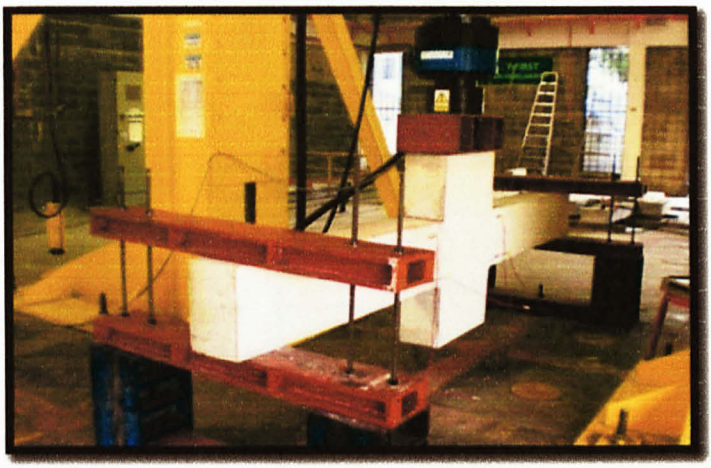

Final experimental setup

Appendix B. Results of static load test on beam column joint sample

Actuator: 1 Channel:0 A1 Load : Current (kN)	Actuator: 1 Channel:1 A1 Stroke : Current (mm)
0.17	1.4200
3.98	3.5765
8.01	5.8319
12.16	8.6217
16.18	11.3233
20.19	13.6605
24.20	15.7652
28.20	17.7927
32.21	19.8878
36.21	22.4869
40.20	25.4139
44.20	30.7274
44.61	32.2212
44.66	32.6876
44.66	32.9601
44.66	33.1383
44.66	33.2581
44.66	33.3627
44.66	33.4374
45.10	33.5508
48.99	39.0383
51.91	60.2353
16.04	58.3400
16.04	58.2988
16.04	58.2801
16.04	58.2684

Appendix C

Modified Mercalli Intensity Scale of 1931 (Abridged)

I. Not felt. Marginal and long-period effects of large earthquakes.

II. Felt by persons at rest, on upper floors, or favorably placed.

III. Felt indoors. Hanging objects swing. Vibration like passing of light trucks. Duration estimated. May not be recognized as an earthquake.

IV. Hanging objects swing. Vibration like passing of heavy trucks; or sensation of a jolt like a heavy ball striking the walls. Standing motor cars rock. Windows, dishes, doors rattle. Glasses clink. Crockery clashes. In the upper range of IV, wooden walls and frame creak.

V. Felt outdoors; direction estimated. Sleepers wakened. Liquids disturbed, some spilled. Small unstable objects displaced or upset. Doors swing, close, open. Shutters, pictures move. Pendulum clocks stop, start, change rate.

VI. Felt by all. Many frightened and run outdoors. Persons walk unsteadily. Windows, dishes, glassware broken. Knickknacks, books, etc., off shelves. Pictures off walls. Furniture moved or overturned. Weak plaster and masonry D cracked. Small bells ring (church, school). Trees, bushes shaken (visibly, or heard to rustle.

VII. Difficult to stand. Noticed by drivers of motor cars. Hanging objects quiver. Furniture broken. Damage to weak masonry D, including cracks. Weak chimneys broken at roof line. Fall of plaster, loose bricks, stones, tiles, cornices. Some cracks in masonry C. Waves on ponds; water turbid with mod. Small slides and caving in along sand or gravel banks. Large bells ring. Concrete irrigation ditches damaged.

VIII. Steering of motor cars affected. Damage to masonry C; partial collapse. Some damage to good masonry B; none to masonry A. Fall of stucco and some masonry walls. Twisting, fall of chimneys, factory stacks, monuments, towers, elevated tanks. Frame houses moved on foundations if not bolted down; loose panel walls thrown out. Decayed piling broken off. Branches broken from trees. Changes in flow or temperature of springs and wells. Cracks in wet ground and on steep slopes.

IX. General panic. Masonry D destroyed; masonry C heavily damaged, sometimes with complete collapse; masonry B seriously damaged. Frame structures, if not bolted, shifted off foundation. Frames racked. Serious damage to reservoirs.

Appendix D. Richter scale

Richter Magnitudes	Description	Earthquake Effects	Frequency of Occurrence
Less than 2.0	Micro	Microearthquakes, not felt.	About 8,000 per day
2.0-2.9	Minor	Generally not felt, but recorded.	About 1,000 per day
3.0-3.9	Minor	Often felt, but rarely causes damage.	49,000 per year (est.)
4.0-4.9	Light	Noticeable shaking of indoor items, rattling noises. Significant damage unlikely.	6,200 per year (est.)
5.0-5.9	Moderate	Can cause major damage to poorly constructed buildings over small regions. At most slight damage to well-designed buildings.	800 per year
6.0-6.9	Strong	Can be destructive in areas up to about 160 kilometres (100 mi) across in populated areas.	120 per year
7.0-7.9	Major	Can cause serious damage over larger areas.	18 per year
8.0-8.9	Great	Can cause serious damage in areas several hundred miles across.	1 per year
9.0-9.9	Great	Devastating in areas several thousand miles across.	1 per 20 years
10.0+	Epic	Never recorded; see below for equivalent seismic energy yield.	Extremely rare (Unknown)

Appendix E. Non-numerical comparison between Mercalli Intensity and Richter Scale

Mercalli Intensity Scale	Richter Scale
I	<3.5
II	3.5
III	4.2
IV	4.5
V	4.8
VI	5.4
VII	6.1
VIII	6.5
IX	6.9
X	7.3
XI	8.1
XII	>8.1